RJC

RASĀYAN *J. Chem.*
Vol. 18 | No. 3 |1414-1422| July-September | 2025
ISSN: 0974-1496 | e-ISSN: 0976-0083 | CODEN: RJCABP
http://www.rasayanjournal.com
http://www.rasayanjournal.co.in

# EVALUATION OF ANTI-CORROSIVE EFFECT OF THIOUREA ON MS IMMERSED IN SODIUM CHLORIDE SOLUTION

**M. Anitha, G. Nivetha, R. Banumathi, R. Abdul Vahith, S. S. Syed Abuthahir✉ and H. Mohamed Kasim Sheit**

PG and Research Department of Chemistry, Jamal Mohamed College (Autonomous), Affiliated to Bharathidasan University, Tiruchirappalli-620 020, Tamil Nadu, India.
✉Corresponding author: syedchemjmc@gmail.com

**ABSTRACT**

Sodium chloride and thiourea: how they interact loss of mass at ambient temperature was used to evaluate corrosion in MS. Corrosion and inhibition were shown by weight loss. Rust is reduced by increasing the concentration of inhibitors. Increased inhibitor concentration leads to better corrosion inhibition. The active site of MS is blocked and protected at higher doses of inhibitor solutions. The growth of the MS protective layer was evaluated in analytical experiments. This investigation employed alternating current impedance spectra and potentiodynamic polarization. Subsequently, SEM and FTIR confirm these results. Elements on the external surface of MS were investigated using EDAX both with and without an inhibitor, after immersion in sodium chloride. SEM tests the degree of surface smoothness in corroded, polished, and inhibitor systems MS.

**Keywords:** Corrosion, MS, EDAX, Thiourea, Sodium Chloride.

RASĀYAN *J. Chem.*, Vol. 18, No. 3, 2025

## INTRODUCTION

Corrosion occurs when an object interacts chemically or electrochemically with its environment. The corrosion process may alter the properties of iron and even ruin it if left unchecked. Metal atoms lose electrons during corrosion, which is caused by oxidation. Early corrosion research is dominated by electrochemical investigations. Corrosion slashes material value in half. Over time, exposure to the elements causes corrosion in both metals and non-metals. Physical buildings and infrastructure are profoundly impacted by this dynamic. Surfaces made of steel rust when they come into contact with oxygen and water. How quickly underground structures and pipes deteriorate is dependent on soil chemistry and moisture. Changes in electrochemical potential, pH, metal cation migration into the coating matrix, and oxide growth are all factors to be considered. Corrosion of carbon steel and iron is an important issue with both theoretical and practical implications.[1] Equipment and structures are affected by corrosion in more ways than one, and the impacts of corrosion go beyond the mere reduction of metal mass. There are a number of failures and expensive replacements that may happen even with little metal damage.[2] Metals degrade due to corrosion, which occurs when they react chemically with their surroundings. Resolving this persistent problem is a challenging and costly endeavor. However, inhibitors may lessen rusting. Oxides, hydroxides, and sulfides are the byproducts of natural corrosion that turn pure metals into them. Through a series of chemical and electrochemical reactions with their environment, this process deteriorates materials, primarily metals.[3] Organic molecules with a functional group at their adsorption active core constitute the vast majority of inhibitors used in industry.[4-5] Here we take a look at thiourea's corrosion resistance in MS in a sodium chloride solution. The efficacy of corrosion and inhibition was assessed using weight loss measurement. The external layer of the MS was scrutinized through SEM and FTIR methodologies, while the electrochemical corrosion phenomena were explored utilizing PDP and AC impedance spectroscopy techniques. The MS surface was anticipated to exhibit a greater degree of refinement compared to both the inhibitor and non-inhibitor models.

## EXPERIMENTAL

A technique to reduce weight was carried out on MS specimens that measured 1.0 cm × 4.0 cm × 0.2 cm. The samples were washed with acetone to remove any grease and polished to obtain a highly reflective surface. They consisted of 0.026%- S, 0.068%- P, 0.36%- Mn, 0.13%- C, and the remaining material was Fe.


http://doi.org/10.31788/RJC.2025.1839232

**Weight Loss Method**

Following the procedure outlined in earlier references [6-10]. MS specimens were engrossed in a water solution covering 60 ppm Cl for 24 hours, both with and without inhibitor concentrations ranging from 50 ppm to 250 ppm. The weight loss measurements were then recorded. After the allotted time had passed, the specimen was carefully removed, rinsed, dehydrated, and then pondered. The formula for corrosion inhibition efficiency (IE) was:

$$IE= (W_1-W_2)/ W_1\times100\%$$

$W_1$ signifies the mass loss without the inhibitor, while $W_2$ indicates the mass loss with the inhibitor present.

**Potentiodynamic Polarization**

In order to investigate polarization, an electrochemical workstation impedance analyzer (CHI 660A) manufactured by H&CH in Austin, United States of America, was used. This experiment used an electrochemical battery that had three electrodes. The task was carried out using electrodes that had a surface area of one centimeter squared and were composed of red lacquered mild steel (MS). An electrode made of saturated calomel (SCE) served as the reference electrode, while a foil made of platinum rectangular shape served as the counter electrode. The experiments maintained a constant potential because the working electrode was smaller. Key parameters, including corrosion potential, linear polarization resistance (LPR), and Tafel slopes, were determined during the experiment. We put the platinum and functioning electrodes in seawater, with and without an inhibitor, to see what happened. Salinity bridged the gap between the test fluid and the saturated calomel electrode. We plotted E, the potential, versus I, the logarithm of current.[11,12]

**Impedance Spectra**

The equipment utilized to generate the impedance spectra was quite comparable to that used for the polarization experiment. In line with previous potentiodynamic polarization experiments, the cell configuration was kept constant. We conducted measurements of the cell impedance at numerous frequencies, considering both the actual and imaginary components (Z' and Z", respectively). The initial values of E (v) were set to 0V. The high and low frequencies were set to 1×105 Hz and 1 Hz, respectively. A 0.005 V signal amplitude and 2-second settling time were employed to gather AC impedance data. Calculations included $C_{dl}$ and $R_t$.[13,14]

$$C_{dl}= ½\ \pi.R_t.f_{max}$$

Where $f_{max}$ denotes the maximum frequency.

**Surface Texture**

For one day, several test solutions were used to immerse the MS specimens. The next step was to dry the MS specimens completely after removal. The layer that developed on the MS specimen's surface was examined using a variety of surface examination methods.

**FTIR Spectra**

Utilizing a spectrophotometer that adheres to the Perkin Elmer Spectrum Version format, Fourier transform infrared spectra were acquired. Pellets were prepared by removing the film and combining them with KBr. Next, we recorded FTIR spectra. Following an extensive period of exposure to different environments, the specimens were carefully extracted from the test fluids and left to dry. The top layer was carefully scraped and blended to ensure a consistent and even texture.[15,16]

**SEM**

The MS specimen was in blank and inhibitor solutions all day. We then washed it twice with distilled water, dehydrated it, and inspected the surface morphology under a SEM. The MS surface morphology was measured using a Tescan Vega 3 computer-controlled SEM.[17,18]

**EDAX**

For one day, the MS specimen was immersed in liquids containing inhibitors and blanks. The MS surface components were determined by cleaning it with double-distilled water, drying it, and then examining it in an EDAX after removal.[19,20] Components of the MS surface were evaluated using Bruckner's computer-

controlled EDAX (Bruckner, Nano, GMBH, Germany).

## RESULTS AND DISCUSSION

### Evaluation of the Weight Loss Technique

Table-1 presents the corrosion rates of mild steel in a 60-ppm chloride aqueous solution, together with the inhibition efficiency (IE) with and without thiourea, assessed by weight loss. At 250 ppm thiourea, observational evidence reveals 74.50% inhibitory efficacy. Table-1 shows that thiourea inhibits. Ionization efficiency is 74.50%, and concentration is 250 ppm for thiourea. IE increases proportionally to thiourea. The higher inhibitor concentration covers more surface area, reducing MS dissolution. N and S atoms' electron-donating properties and delocalized π-electrons contribute to higher inhibitory efficiency. Several studies support this monitoring.[21,22]

Table-1: Tabulation of Weight Loss Technique

| $Cl^-$ (ppm) | Thiourea (ppm) | CR (mdd) | IE (%) |
|---|---|---|---|
| 60 | 0 | 70.19 | _ |
| 60 | 50 | 39.40 | 47.56 |
| 60 | 100 | 29.32 | 60.19 |
| 60 | 150 | 25.59 | 69.78 |
| 60 | 200 | 20.14 | 70.52 |
| 60 | 250 | 17.28 | 82.90 |

### Analysis of Results of PDP

A defensive coating may be successfully applied to MS in order to decrease corrosion, according to polarization studies.[23-25] The development of a shielding coating on MS results in an improvement in its corrosion potential, current, and linear polarization resistance (LPR). Figure-1 shows MS PDP curves in 60 ppm Cl- water with and without an inhibitor. Table-2 shows corrosion parameters. MS corrosion potential against SCE was -508 mV. The combination with 250 ppm thiourea had a noble corrosion potential of -459 mV vs SCE. There seems to be a protective layer at MS anodic sites. The film creates a Fe2+-thiourea combination on the anodic sites of MS surfaces, which regulates the steel's degradation. LPR rises from 174096.1 to 174198.8 ohm $cm^2$. The corrosion current shows a reduction from $2.433 \times 10^{-7}$ A/cm² to $2.412 \times 10^{-7}$ A/cm² under an 8-ohm cm² condition. The protective layer of MS is shown by the polarization investigations.

Table-2: PDP Parameters

| Systems | $E_{corr}$ Vs SCE (mV) | $I_{corr}$ ($A/cm^2$) | $b_a$ (mV/dec) | $b_c$ (mV/dec) | LPR (ohm $cm^2$) |
|---|---|---|---|---|---|
| 60 ppm $Cl^-$ | - 508 | $2.433\times 10^{-7}$ | 186 | 206 | 174096.1 |
| 60 ppm $Cl^-$ + 250 ppm thiourea | - 459 | $2.412 \times 10^{-7}$ | 195 | 264 | 174198.8 |

### Examination of Results of Impedance Spectra

The confirmation of a protective coating on MS can be achieved through electrochemical impedance spectra (AC). The application of protective layers on MS has resulted in numerous alterations. The increase in surface resistivity correlates with a rise in charge transfer resistance. Furthermore, there is a reduction in double-layer capacitance (Cdl), suggesting a decline in charge storage capacity. An ascending impedance logarithm (z/ohm) indicates more impedance.[26–28] Figure-2 presents Nyquist plots of MS impedance spectra in a 60 ppm $Cl^-$ solution, both with and without malic acid (a, b). Figure-3(a, b) presents pertinent Bode graphs. The parameters of AC impedance encompass double-layer capacitance (Cdl) and charge transfer resistance ($R_t$), as detailed in Table-3.

The Rt increases from 518.1 Ω cm² to 754.1 Ω cm² with the addition of 250 ppm thiourea inhibitor. Simultaneously, Cdl decreases to $2.81 \times 10^{-4}$ F $cm^{-2}$ from $6.13 \times 10^{-3}$ F $cm^{-2}$. The phase angle rises from 25° to 27°, along with an increase in impedance from 0.501 to 0.505. The data suggest that the corrosion resistance of MS may be enhanced with a protective coating.

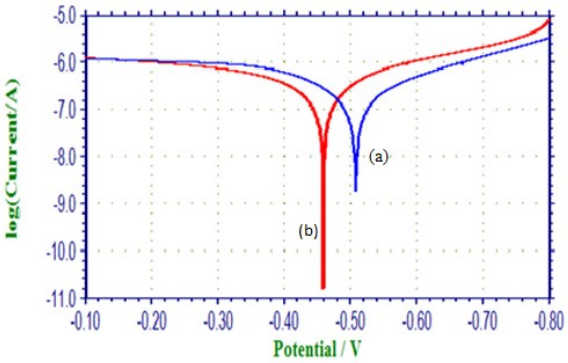


Fig.-1: PDP curves of MS in Test Solutions (a)60ppm of $Cl^-$ , (b) 60ppm of $Cl^-$ + Thiourea (250 ppm)

Table-3: Electrochemical Impedance

| Systems | Nyquist plot | | Bode plot |
|---|---|---|---|
| | $R_t$ $\Omega$ $cm^2$ | $C_{dl}$ F $cm^{-2}$ | Impedance Lg ( Z $ohm^{-1}$) |
| 60 ppm $Cl^-$ | 518.1 | $6.13 \times 10^{-3}$ | 0.501 |
| 60 ppm $Cl^-$ + 250 ppm thiourea | 754.1 | $2.81 \times 10^{-4}$ | 0.505 |

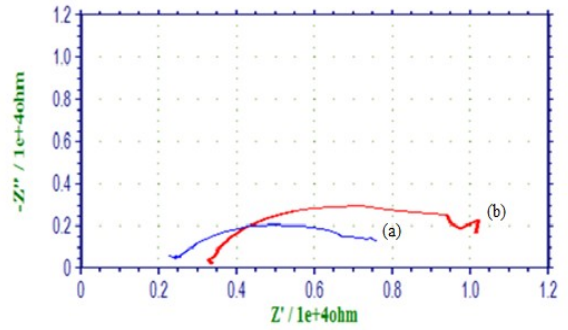


Fig.-2: AC Impedance Spectra Nyquist Plots for MS in Test Solutions
(a) 60 ppm $Cl^-$ (b) 60 ppm $Cl^-$ with 250 ppm Thiourea

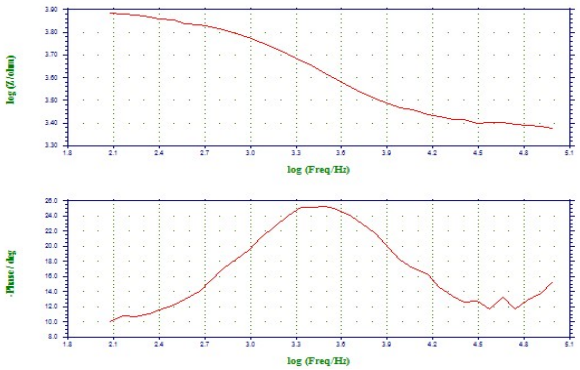


Fig.-3a: Bode Plot of 60 ppm of Cl

## FTIR Spectra

Fourier transform infrared spectra were employed to investigate the protective layer of MS. The molecular structure of thiourea is illustrated in Fig.-4. The FTIR spectrum of thiourea in water (KBr) is presented in Fig.-5a. The bond length between carbon and sulfur is measured at 1107.59 $cm^{-1}$. The primary nitrogen peaks are observed at 3410.20 $cm^{-1}$, while the carbon-nitrogen bonds exhibit a peak at 1480.33 $cm^{-1}$.

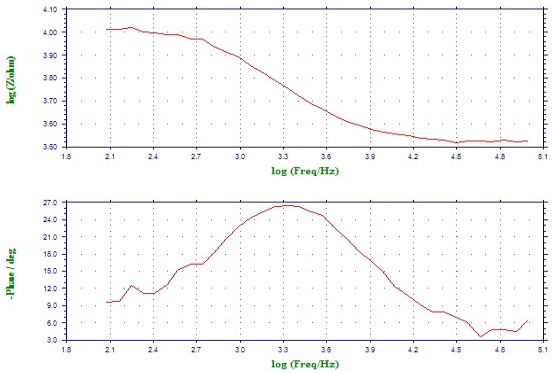


Fig.-3b: Bode Plot of 60 ppm of $Cl^-$ + 250 ppm of Thiourea

Figure-5b displays the FTIR spectrum of the carbon steel coating (KBr) following exposure to 60 ppm $Cl^-$ and 250 ppm thiourea in water. The C=S stretching frequency was altered between 1107.59 $cm^{-1}$ and 1020.72 $cm^{-1}$. A main nitrogen signal is seen at 3413.84 $cm^{-1}$. Peak absorption at the C-N bond transitioned from 1480.33 to 1423.87 $cm^{-1}$. The results show that thiourea's sulfur and nitrogen atoms have formed a film on MS by coupling with $Fe^{2+}$. A $Fe^{2+}$-thiourea compound is shown to be the protective layer by FTIR.[29-32]

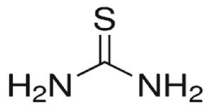


Fig.-4

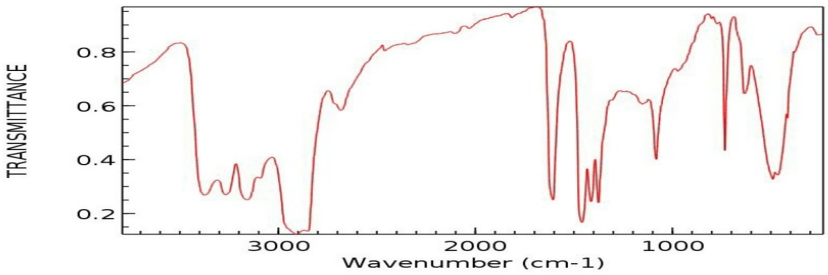


Fig.-5a: FTIR Spectra of Pure Thiourea

**SEM**

Pictured here is the surface in a scanning electron micrograph. A thorough examination of surface scanning electron micrographs has been conducted in order to comprehend the surface layer and the impact of inhibitors on MS corrosion.[33-37] Pictures of an MS specimen submerged in a 60 ppm $Cl^-$aqueous solution for one day are shown in SEM pictures in Fig.-6a, 6b, and 6c. Before and after the inhibitor system is applied, the specimen is shown in the photographs. The control surface, which is polished MS, is shown in Fig.-6a with scanning electron micrographs, demonstrating its smoothness. There are no inhibitor complexes or corrosion products seen on MS. Figure-6b is a scanning electron micrograph (SEM) of an MS surface immersed in a 60 ppm $Cl^-$ aqueous solution; the surface is rough, indicating a severely corroded area. Figure-6c shows a decrease in damaged areas, indicating that corrosion is inhibited at 250 ppm of thiourea. Because of an insoluble component, MS almost always corrodes.[38] Through the formation of a surface inhibitor layer, thiourea regulates the MS degradation process.

**EDAX**

EDAX survey spectra were used to investigate MS surface elements before and after inhibitor solution exposure.[39-40] MS sample surfaces were analyzed with and without inhibitors using EDAX. Figure-7a shows MS's EDAX spectrum, whereas Figure-7b shows its behavior in 60 ppm $Cl^-$ aqueous solution. The MS sample has element-specific peaks. MS's EDAX spectra in 60 ppm $Cl^-$ and 250 ppm thiourea aqueous solution are publicised in Fig.-7c. Additional line drops for O signals and rises for Fe signals. Inhibitors boost Fe and O signals.

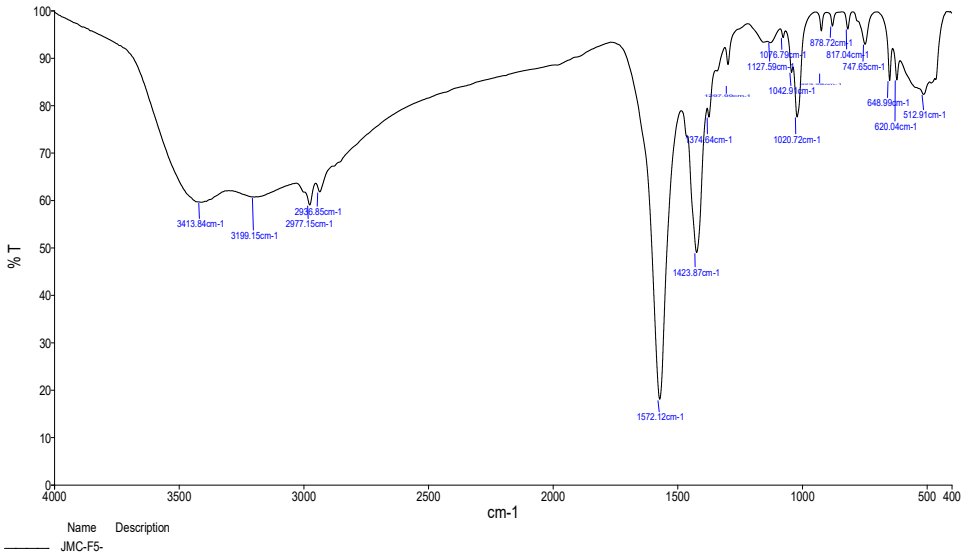


Fig.-5b: The FTIR Spectrum -60 ppm $Cl^-$ with 250 ppm of Thiourea

Statistics show that MS's surface comprises Fe, S, C, P, and Mn. This layer is evidently a result of the inhibitor system. An aqueous solution with 60 ppm $Cl^-$ shows no Fe, Mn, O, or C signals on the MS surface. Figure-7c shows that an inhibitor greatly lowers Fe peak intensity relative to the blank solution with 60 ppm $Cl^-$.

The top inhibitor film suppresses Fe peaks. It seems that steel is protected from corrosion by an adsorbed inhibitor layer. The findings indicate that thiourea's O, N, and C atoms coordinate with $Fe^{2+}$ ions. MS forms a $Fe^{2+}$-thiourea complex due to this interaction.

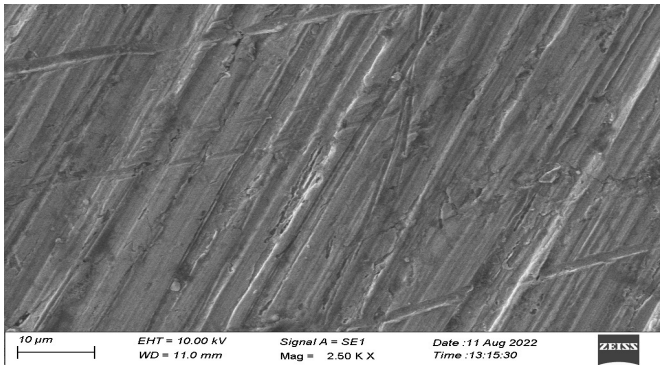


Fig.-6a: SEM (blank)

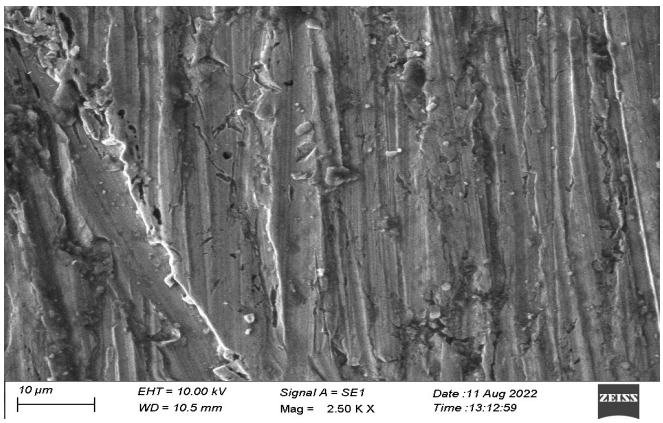


Fig.-6b: SEM MS Specimen

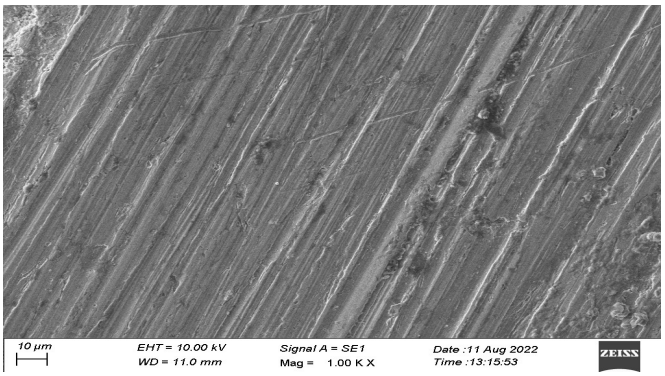


Fig.-6c: SEM-MS with 250 ppm of Thiourea

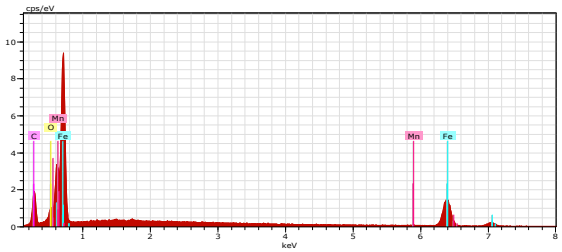


Fig.-7a: EDAX Spectrum (control)

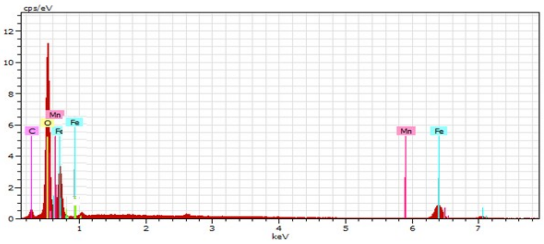


Fig.-7b: EDAX Spectrum (blank)

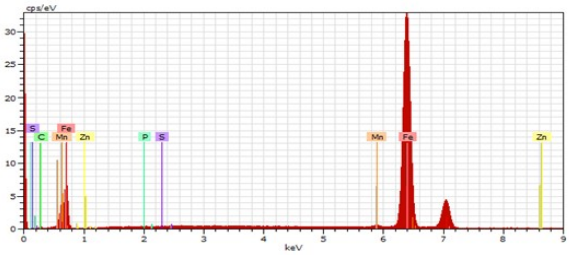


Fig.-7c: EDAX Spectrum - 60 ppm of $Cl^-$ + 250 ppm of Thiourea

## CONCLUSION

Thiourea inhibited MS corrosion in a 60 ppm $Cl^-$ aqueous solution in this investigation. Analysis of weight loss, polarization, impedance, and surface investigation methods like FTIR and SEM explains corrosion inhibition mechanistic features. EDAX survey spectra were used to investigate MS surface elements before and after inhibitor solution exposure. The addition of organic substances slows corrosion, possibly because thiourea clings to metal. The maximum inhibition effectiveness was 82.90%. The present research suggests the following. Thiourea, when dissolved in water with 60 ppm Cl-, effectively prevents the corrosion of MS. The weight reduction strategy works by inhibiting at 82.90%. Anodic reactions are hindered by thiourea complexes, according to the polarization study. The relationship between $R_t$, $C_{dl}$, and $I_{corr}$, the corrosion current, has been shown in electrochemical impedance tests. Because the adsorbed layer is thicker. Based on the FTIR spectra, the protective layer is a molecule called $Fe^{2+}$-thiourea. With and without an inhibitor, SEM was used to analyze the microstructure of MS. Thiourea prevents MS corrosion when dissolved in sodium chloride. Both the pre- and post-exposure to the inhibitor solution EDAX spectra confirmed the surface components of the MS.

## ACKNOWLEDGMENTS

The authors are thankful to the Principal and the College Management Committee Members of Jamal Mohamed College (Autonomous), for providing necessary facilities. The authors are also thankful to the DBT and DST-FIST for providing instrumental facilities to carry out research work.

## CONFLICT OF INTERESTS

The authors declare that there is no conflict of interest.

## AUTHOR CONTRIBUTIONS

The present work is related to *SDG-9: Industry, Innovation and Infrastructure*. All the authors contributed significantly to this manuscript, participated in reviewing/editing and approved the final draft for publication. The research profile of the authors can be verified from their ORCID ids, given below:

M. Anitha https://orcid.org/0009-0004-0304-6159
G. Nivetha https://orcid.org/0000-0002-8165-2152
R. Banumathi https://orcid.org/0009-0000-0461-6732
R. Abdul Vahith https://orcid.org/0009-0009-9750-5235
S.S. Syed Abuthahir https://orcid.org/0000-0002-7872-0943
H. Mohamed Kasim Sheit https://orcid.org/0000-0003-2060-316X



## REFERENCES

1. R.W. Revie, and H.H. Uhlig, *Corrosion Science*, **30**, 973(1990), https://doi.org/10.1016/0010-938X(90)90002-W.
2. F. Mansfeld, *Corrosion Science*,**16**, 573(1976), https://doi.org/10.1016/0010-938X(76)90004-8
3. D. A. Jones, *Journal of The Electrochemical Society*, **122**, 280(1975), https://doi.org/10.1149/1.2134217.
4. R. Fuchs-Godec, *Materials Chemistry and Physics*, **95**, 256(2006), https://doi.org/10.1016/j.matchemphys.2005.06.045.
5. N. Hackerman, *Langmuir*, **3**, 922(1987), https://doi.org/10.1021/la00078a009.
6. K.F. Khaled, *Electrochimica Acta,* **48**, 2493(2003), https://doi.org/10.1016/S0013-4686(03)00306-1.
7. I. Garcia-Santos, J. Sanmartin, A.M. Garcia-Deibe, M. Fondo and E. Gomez, *Inorganica Chimica Acta*, **363**, 193(2010), https://doi.org/10.1016/j.ica.2009.09.004.
8. M. Albrecht, K. Witt, P. Weis, E. Wegelius and R. Frohlich, *Inorganica Chimica Acta*, **341**, 25(2002), https://doi.org/10.1016/S0020-1693(02)01201-X.
9. S. Rajendran, B.V. Apparao and N. Palaniswamy, *Bulletin of Electrochemistry*, **17**, 141(2001).
10. R.B. Rastogi, M.M. Singh, K. Singh and M. Yadav, *Portugaliae Electrochimica Acta*, **22**, 315(2005).
11. A.K. Dubey and G. Singh, *Electrochimica Acta*, **25**, 221(2007).
12. I.A. Akpan and N.A.O. Offiong, *International Journal of Corrosion*, **1**, 301689(2013), https://doi.org/10.1155/2013/301689.
13. M.F. Montemor, *Surface and Coatings Technology*, **258**, 17(2014), https://doi.org/10.1016/j.surfcoat.2014.06.03.
14. E. Venereau, C. Diveu, L. Grimaud, E. Ravon, J. Froger, L. Preisser and H. Gascan, *Journal of Biological Chemistry*, **285**, 14955(2010), https://doi.org/10.1074/jbc.M109.049163.
15. M. Adamu, L.E. Umoru and O.O. Ige, *Journal of Minerals & Materials Characterization & Engineering*, **2**, 1(2014), https://doi.org/10.4236/jmmce.2014.21001.
16. E.C. Chinwko, B.O. Odio, J.L. Chukwuneke and J.E. Sinebe, *International Journal of Scientific and Technology Research*, **3**, 306(2014).
17. M. Manivannan and S. Rajendran, *International Journal of Engineering Science and Technology*, **3**, 19(2011).

18. V. Johnsirani, S. Rajendran, J. Sathiyabama, T.S. Muthumegala, A. Krishnaveni and N. Hajara Beevi, *Bulgarian Chemical Communications*, **44**, 41(2012).
19. H.M.K. Sheit, M.S. Mubarak and G. Benitta, *Journal of Bio- and Tribo-Corrosion*, **8**, 103(2022), https://doi.org/10.1007/s40735-022-00746-w.
20. H.T.M. Abdel-Fatah, *Anti-Corrosion Methods and Materials*, **59**, 23(2012), https://doi.org/10.1108/00035591211199438.
21. C.M. Anbarasi and S. Rajendran, *Journal of Electrochemical Science and Engineering*, **2**, 1(2012), https://doi.org/10.5599/jese.2012.0012.
22. H.H. Abdel Rahman, A.H.E. Moustafa and M.K. Awad, *International Journal of Electrochemical Science,***7**, 1266(2012), https://doi.org/10.20964/2012.02.33.
23. M. Behpour, S.M. Ghoreishi, A. Gandomi-Niasar, N. Soltani and M. Salavati-Niasari, *Journal of Materials Science*, **44**, 2444(2009), https://doi.org/10.1007/s10853-009-3284-2.
24. R. Manickavasagam, K.J. Karthik, M. Paramasivam and S.V. Iyer, *Anti-Corrosion Methods and Materials*, **49**, 19(2002), https://doi.org/10.1108/00035590210415397.
25. T.A. Aliev, *Materials Science*, **44**, 665(2008), https://doi.org/10.1007/s11003-009-9118-0.
26. W.A. Badawy, K.M. Ismail and A.M. Fathi, *Electrochimica Acta*, **51**, 4182(2006), https://doi.org/10.1016/j.electacta.2005.12.025.
27. M.S. Morad, *Journal of Applied Electrochemistry*, **38**, 1509(2008), https://doi.org/10.1007/s10800-008-9602-9.
28. O. Olivares-Xometl, N.V. Likhanova, M.A. Domínguez-Aguilar, E. Arce, H. Dorantes and P. Arellanes-Lozada, *Materials Chemistry and Physics*, **110**, 344(2008), https://doi.org/10.1016/j.matchemphys.2008.01.029.
29. N.O. Eddy, *Journal of Advanced Research*, **2**, 35(2011), https://doi.org/10.1016/j.jare.2010.05.004.
30. H.M.K. Sheit, S.M. Kani and M.A. Sathiq, *Results in Surfaces and Interfaces*, **12**, 100143(2023), https://doi.org/10.1016/j.rintsfi.2023.100143.
31. A. Peter and S.K. Sharma, *International Journal of Corrosion and Scale Inhibition*, **6**, 112(2017), https://doi.org/10.17675/2305-6894-2017-6-2-4.
32. Mohamed, K.S.H. Raja. M, *Materials Protection,* **64**, 452 (2023).
33. H.M.K. Sheit, K.S. Mohan, P. Srinivasan, *Results in Chemistry*, **12,** 101894(2024), https://doi.org/10.1016/j.rechem.2023.101894.
34. H.M.K. Sheit, S.M. Kani, M.A. Sathiq, S.S. Abuthahir, P. Subhapriya, K.S. Nivedhitha and A.S. Shaik, *Materials*, **17**, 751(2024), https://doi.org/10.3390/ma17030751.
35. H.M.K. Sheit, M.A. Sathiq, K.S. Mohan, *High Temperature Corrosion of Materials*, **101**, 351(2024), https://doi.org/10.1016/j.htcm.2023.351.
36. P. Mahalakshmi, S. Rajendran, G. Nandhini, S.C. Joycee, N. Vijaya, T. Umasankareswari and N. Renuga Devi, *International Journal of Corrosion and Scale Inhibition*, **9**, 706(2020), https://doi.org/10.17675/2305-6894-2020-9-2-22.
37. W.M.K.W.M. Ikhmal, M.Y.N. Yasmin, M.F.F. Mari, S.M.S. Syaizwadi, W.A.W. Rafizah, M.G.M. Sabri and B.M. Zahid, *International Journal of Corrosion and Scale Inhibition*, **9**, 118(2020), https://doi.org/10.17675/2305-6894-2020-9-1-7.
38. H.M.K. Sheit, M. Seeni Mubarak, K. Mohan, K. Gunavathy, P. Subhapriya and M. Varusai Mohamed, *Zeitschrift für Physikalische Chemie*, **239(2-3)**, (2024), https://doi.org/10.1515/zpch-2023-0410.
39. A. Grace Baby, S. Rajendran, V. Johnsirani, A. Al-Hashem, N. Karthiga and P. Nivetha, *International Journal of Corrosion and Scale Inhibition,* **9**, 979(2020), https://doi.org/10.17675/2305-6894-2020-9-3-23.
40. S. Rajendran, R. Srinivasan, R. Dorothy, T. Umasankareswari and A. Al-Hashem, *International Journal of Corrosion and Scale Inhibition*, **8**, 437(2019), https://doi.org/10.17675/2305-6894-2019-8-3-14.

[RJC-9232/2025]